The Impact of Independently Derived Neutral Winds on Ionospheric Frictional Heating

A. M. Pepper[1] and S. R. Kaeppler[1]

1. Department of Physics and Astronomy, Clemson University, Clemson, SC, 29634

Abstract

Closure of field-aligned currents in the E-region ionosphere occurs through Hall and Pedersen currents which are set up because of ion-neutral collisions that allow ions to drift perpendicular to the mean magnetic field. Joule heating is a combination of the Pedersen conductivity and the electric field in the frame of the neutral winds and represents a sink of magnetospheric energy. The Pedersen conductivity, perpendicular electric field, and neutral winds have different dependencies on magnetic local time (MLT) and level of geomagnetic activity. The neutral wind profile is a particularly challenging aspect in the calculation of Joule heating. The most successful technique for producing altitude-resolved wind measurements is the chemical tracer technique, although other techniques using incoherent scatter radar have been developed. Previous ISR investigations have shown that the neutral wind can enhance or reduce energy deposition in both case studies and statistical investigations spanning MLT. We present Joule heating rates with and without the thermospheric profiles as well as other related energy exchange parameters derived using the aforementioned datasets. We find the impact of the neutral wind varies depending on the geomagnetic conditions and impacts the amount of energy deposited by either enhancing or inhibiting frictional heating with the most significant variation found during the dusk sector. We find that without enhancements in geomagnetic activity ($Kp \leq 2$), the inclusion of neutral wind increases the Joule heating rate by up to 25%. In contrast, with enhancements in geomagnetic activity ($Kp \geq 2$) and the inclusion of the neutral wind, the Joule heating rate is reduced by up to 36%.

Campaign	DOL	TOL (UT)	MLT Sector	Kp	Upleg TMA Range	Downleg TMA Range	Ne	E
Joule 1	3/27/2003	12:09	post-midnight	3.3	95-134 km	94-160 km	LP	DC Probes
Joule 1	3/27/2003	12:12	post-midnight	3.3	95-134 km	94-160 km	LP	DC Probes
Joule 2	1/19/2007	12:29	post-midnight	2.6	95-140 km	92-129 km	LP/ PFISR	DC Probes
Joule 2	1/19/2007	12:45	post-midnight	2.6	95-140 km	92-129 km	LP/ PFISR	DC Probes
Auroral Jets (low)	3/2/2017	5:41	dusk	4.3	102-187 km	98-183 km	PFISR	DC Probes
Auroral Jets (high)	3/2/2017	5:42	dusk	4.3	102-187 km	98-183 km	PFISR	DC Probes
INCAA	4/7/2022	12:47	post-midnight	2.3	95-170 km	90-168 km	PFISR	DC Probes

Motivation & Methods

❖ **How does the E-region neutral wind impact ionospheric frictional heating?**

❖ The sounding rocket campaigns in this study met three selection criteria: They were launches from the high latitude region with coincident ground-based PFISR and allsky/photometer measurements, they dispersed trimethylaluminum (TMA) at E-region altitudes that were triangulated and processed into a neutral profile, and all had varying levels of geomagnetic activity in different MLT sectors. Information on each campaign is shown in the Table above. The Pedersen conductivity (conductance) was calculated using the equation below which is taken from Section 2.2 in Kelley, 2009. NRLMSIS-2.1 provides the neutral temperatures while PFISR provides both the plasma density and ion temperatures required except when IRI is necessary.

$$\sigma_P = ne^2 / \left[M\nu_{in} \left(1 + \kappa_i^2\right) \right]$$

❖ The source for electric fields used in the calculations of frictional heating are from the DC electric field probes flown during the respective mission and are depicted in figure 1. The vapor trails of TMA were photographed and triangulated to obtain neutral velocity profiles utilizing the line-of-sight projection method providing profiles between 100-140 km which are depicted in figure 2. To investigate the rate of ionospheric frictional heating in the E-region, we may consider two regimes. The Joule heating rate is derived from Ohm's law and includes contributions from the conductivity, electric field, and neutral wind. The second regime is found by setting the neutral component to zero and is known as the passive energy deposition rate which only depends on the northward conductivity and electric field.

$$q_j^E = \sigma_P \mathbf{E}_\perp^2 \qquad q_j = \sigma_P (\mathbf{E}_\perp + \mathbf{U}_n \times \mathbf{B})^2$$

Results

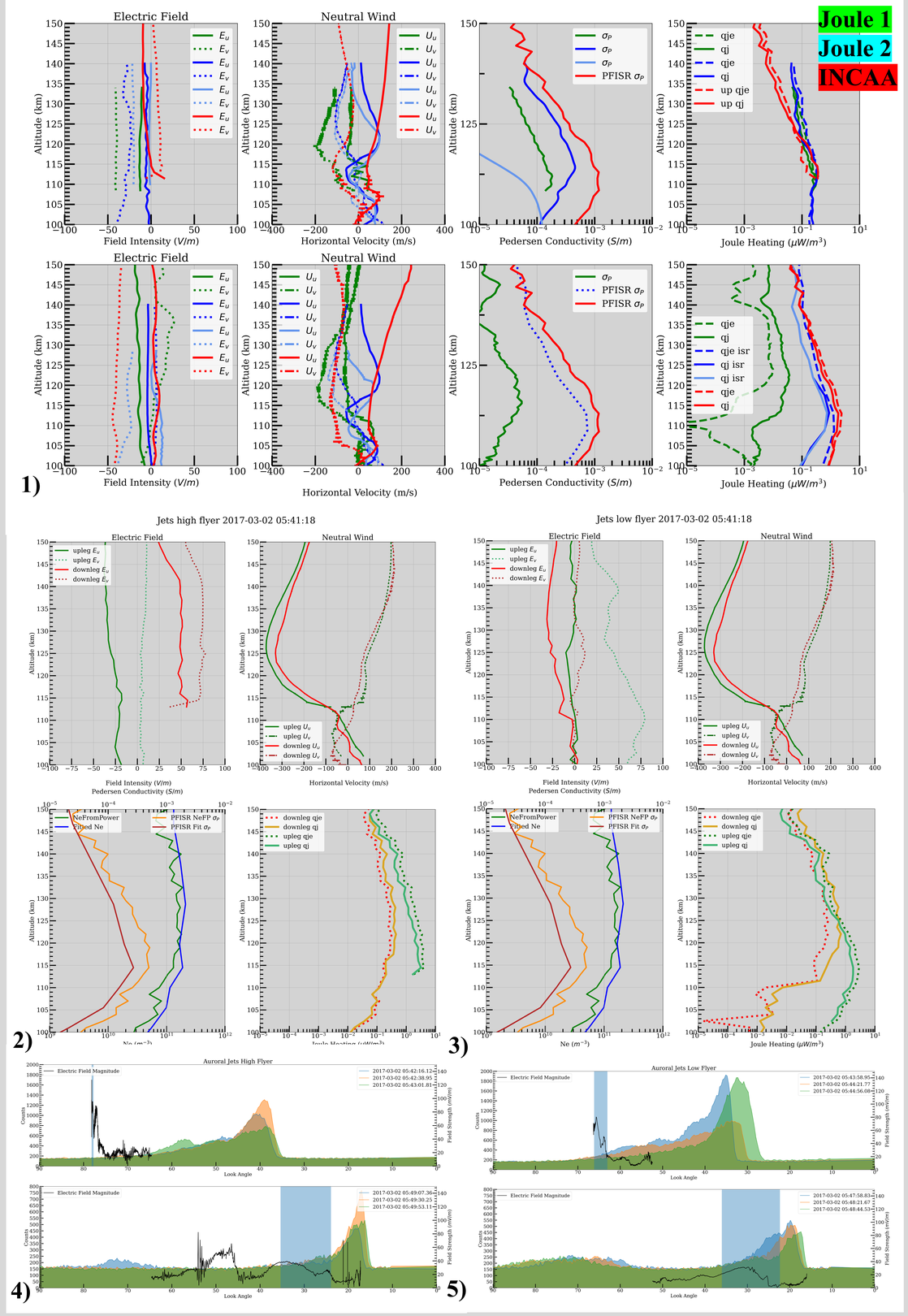

Mission	Trajectory	Σp (mhos)	Qje (mW/m2)	Qj (mW/m2)	Qm (mW/m2)	% diff
Joule 1 (first)	Upleg	3.03	4.1	3.3	2.4	-24%
	Downleg	1.4	0.2	0.75	-1.2	73%
Joule 1 (second)	Upleg	2	5.1	4	0.5	-28%
	Downleg	1.7	0.7	0.6	-0.7	-17%
Joule 2 (first)	Upleg	9.3	7.9	7.4	1.5	-7%
	Downleg	0.7	0.023	0.024	-0.3	4%
Joule 2 (second)	Upleg	1.9	0.8	0.88	0.27	9%
	Downleg	0.7	0.11	0.1	0.25	-10%
Jets (High)	Upleg	10.3	64.9	42.4	18.2	-53%
	Downleg	10.3	8.5	11.1	-17.7	23%
Jets (Low)	Upleg	10.3	36.7	27.1	18.9	-35%
	Downleg	10.3	4.9	7.7	-0.96	36%
INCAA	Upleg	14.6	1.9	2.5	-1.2	24%
	Downleg	14.6	41.2	35.6	7.7	-16%

❖ 1) The compilation of the in-situ based measurements and calculations of the energy exchange parameters for the post-midnight sector launches of the Joule 1, Joule 2, and INCAA missions. All three were launched from Poker Flat research range between 12 UT and 13 UT as indicated in table 1. The top (bottom) row depicts the measurements and calculations during the upleg (downleg) trajectory. In order from column 1 to column 4, the electric fields, horizontal neutral wind, Pedersen conductivity, and Joule heating rate with and without the neutral component are shown. Despite the variability in the winds, drifts, and conductivities, the response of Joule heating is consistent in the upleg and downleg profiles outside of the Joule 1 downleg calculation.

❖ 2) and 3) The in-situ based measurements and calculations made during the Auroral Jets campaign launched from Poker Flat research range in the dusk sector. The conductivities (PFISR calculated) and neutral wind profiles are the same for both figures and calculations. The upleg high-flyer results show the strongest field intensity and consequently the largest percent change of q_j relative to q_j^e. The downleg trajectory of both rockets show that the inclusion of the neutral wind acts to enhance the heating rate by a variable amount.

❖ 4) and 5) show the magnitude of the electric field relative to the intensity measured from the all-sky cameras located at Poker flat relative to the look angle between the ground station and the rocket. When the rocket is on the edge or just outside of the of the auroral arc the increase in Joule heating is much higher than the case when the rocket is within the arc itself. Further, the influence of the neutral wind flips between enhancing frictional heating and reducing it depending on the location of the rocket relative to the arc.

❖ Table 2 shows the height integrated values for passive energy deposition, Joule heating, and mechanical energy transfer rates from each segment of the rocket trajectories for each launch. The influence of neutral wind is readily apparent as the expression of energy deposition fluctuates relative to the geomagnetic conditions.

Conclusions

❖ For each campaign depicted, we quantify the response of energy exchange parameters to independently derived neutral winds which is dependent upon the MLT sector and geomagnetic activity level.

❖ The influence of neutral wind in relation to frictional heating varies with respect to the geomagnetic activity level and proximity to an auroral arc. In agreement with Zhan et al., 2021, during low geomagnetic activity levels neutral winds tend to increase q_j relative to q_j^e at all E-region heights. In more active conditions, neutral winds reduce q_j to compensate for the primary driver of this forcing regime, the electric field.

❖ Evans et al., 1977 found evidence of enhanced currents relative to the proximity of an auroral arc and a minimum of frictional heating within the arc itself. When geomagnetic activity is high or there is proximity to an auroral arc, neutral winds act as a regulatory mechanism, diminishing the energy deposited by frictional heating. In contrast, during low geomagnetic activity or further from an arc, these winds enhance frictional heating.

❖ The peak altitude of energy deposition via frictional heating is sensitive to the level of geomagnetic activity. When the influence of neutral wind begins to inhibit energy deposition, the peak altitude of the Joule heating rate decreases with respect to altitude.

❖ The results depicted in Sangalli et al., 2009 support a peak altitude of 116 km which agree with the regions of enhanced frictional heating in this investigation. The 28% overestimation of frictional heating is also consistent when energy deposition was enhanced.

Acknowledgements: We thank R. Pfaff (PI of Jets) for providing electric field profiles and Miguel Larsen for providing neutral profiles and guidance essential to this study. We also acknowledge NASA grant #80NSSC19K0810 for funding.